Research Article

Flame retarded polyamide-6 composites via in situ polymerization of caprolactam with perylene-3,4,9,10-tetracarboxylic dianhydride

Xue Zhang[1] · Lei Sun[1] · Yingbo Chen[1] · Cuiyu Yin[1] · Dongqing Liu[1] · Ermin Ding[2]

Abstract

Flame retardant polyamide 6 (PA6) composites (PA6/PTCDA) were prepared by in situ polymerization of caprolactam with adding 0.01–2.5 wt% perylene-3,4,9,10-tetracar-boxylic dianhydride (PTCDA). The structure and properties of PA6/PTCDA composites were studied by Fourier transform infrared spectroscopy, X-ray diffraction, differential scanning calorimetry, thermogravimetric analysis, thermal conductivity, and limiting oxygen index (LOI) measurements. The results indicated that the crystallization of the PA6 chains was suppressed with 2.5 wt% PTCDA, and the LOI of the composite was 29.5. At the same time, the addition of PTCDA made the composites form a coke layer in the process of combustion, protecting the flammable components from volatilization and enhanced the flame retardant performance of the composites. This indicated that the PA6/PTCDA composite prepared by in situ polymerization possessed good flame retardant properties.

Keywords Flame retardant · Perylene-3,4,9,10-tetracarboxylic dianhydride · Polyamide 6 · In situ polymerization

1 Introduction

With the continuous development and improvement of science and technology, the research of new materials is becoming more extensive. Polyamide 6 (PA6) has excellent comprehensive properties, such as high mechanical strength, good electrical insulation properties, abrasion resistance, acid resistance, and alkali resistance [1]. Although PA6 based materials are widely used in daily life, low limiting oxygen index (LOI 20-22) greatly limits their application in elaborate fields [2]. Fires caused by PA6 based materials are innumerable and threatens the safety of people. With the continued development of engineering plastics, people have put forward higher requirements (such as strength, thermal stability, etc.) on PA6, and it can no longer meet the actual demand by virtue of inherent materials properties. Therefore, PA6 modification research is getting more and more attention by researchers [3–5]. Especially, of great practical significance is to improve the flame retardant properties of PA6 in order to improve the safety factors of PA6.

There are many types of flame retardants, which can be divided into halogens, nitrogen, halogen-phosphorus, and silicon systems [6]. Different types of flame retardants have different effects on the properties of PA based materials due to their varied flame-retardant mechanisms. However, the halogen-containing flame retardants are not friendly to the environment and have been banned in many countries [7]. Mu et al. [8] have synthesized PA6/MCA by in situ polymerization. The analysis showed that the fire retardant was well dispersed. Hu et al. [9] added decabromodiphenyl oxide and antimony oxide in a PA6 matrix and explored PA6/montmorillonite nanocomposite self-extinguishing properties. At the same time, many researchers have studied compound flame retardants that usually contain different ingredients. The combination of methyl-blocked novolac (MBN) and magnesium hydroxide (Mg(OH)$_2$) has been added to PA6, which eliminates the melting point of PA6

during the combustion process and the flame retardant properties of MBN/MH/PA6 is better than that of adding a single component to PA6 [10]. Alongi et al. [11] discovered that cyclodextrin nanosponges can act as a novel green flame retardants for PA6 and cyclodextrin nanosponges were also applicable for PP and LLDPE. In the presence of acid sources, cyclodextrin nanosponges dehydrate resulting in producing water vapor and assist in the formation of a carbon layer on the surface of the composite. These studies have already shown promising results. Low toxicity, halogen free, and high efficiency is the trend of development for flame retardants.

There are many ways for flame retardants to work, such as increasing the thermal conductivity of the material, combustion products that suppress combustion, or generation of a carbon layer to cut off the outer flame. Carbon nanotubes and graphene have been used to increase the thermal conductivity of PA6 and during combustion of PA6, heat can be quickly transferred to the atmosphere. Xu et al. [12] explored the thermal properties of a single-walled carbon nanotube/polymer composites. Li et al. [13] studied a new type of graphene with a 3D structure, which was added to PA6 to improve thermal conductivity and reduce melt dripping. However, the addition of these materials does not effectively increase the limiting oxygen index of PA6. At present, most of the flame retardants also are inorganic flame retardants, which are not harmful to the environment. However, the use of such flame retardants is typically large. Therefore, this article is devoted to studying how to effectively improve the flame retardant properties of PA6 by adding a small amount of additives. Perylene-3,4,9,10-tetracarboxylic dianhydride (PTCDA) is a type of red powder. It has monoclinic crystals with a melting point higher than 300 °C. The PTCDA molecule is composed of a perylene nuclear group composed of five central C rings, two acids, and an anhydride located at the ends of the perylene ring [14]. There are also few studies on thermal properties of PTCDA. Aromatic ternary copolyimides containing perylene groups were prepared from PTCDA by one-step method at high temperature. Many high performance polymers can be synthesized by using PTCDA as a raw material. Zeng et al. [15] synthesized a novel thermotropic liquid crystal perylene bisimides polyurethane (LCPU) by using PTCDA, hexamethylene diisocyanate (HDI), and PEG-200 as raw materials. The researchers also mixed LCPU and graphene oxide (GO) to form composites and when the LCPU content was 0.7 wt%, its thermal decomposition temperature increased by 30 °C. Iqbal et al. [16] synthesized poly(azomethine imide) by condensation of different raw materials with PTCDA and found that the synthetic material also has excellent thermal properties. Herein, we disclose the first successfully preparation of PA6/PTCDA composites by in situ polymerization. The

chemical structure and flame retardant properties of the composite are studied.

2 Experimental part

2.1 Chemicals and materials

Caprolactam, 6-aminocaproic acid, and PTCDA were purchased from Shanghai Aladdin Company. Anhydrous calcium chloride, formic acid, and sulfuric acid were obtained from Shanghai Reagents Company. All chemicals were used with as received.

2.2 Preparation of PA6/PTCDA composite

A typical procedure for PA6 composites with 1 wt% PTCDA is as follows. Vacuum dried caprolactam (9 g) and 6-aminocaproic acid (1 g) were added to a four-necked flask connected with a condenser. The mixture was heated to melt for 0.5 h with mechanical stirring under a nitrogen atmosphere. Then 0.1 g PTCDA was added into the four-necked flask. At this point, the color of the mixture turned red. The mixture was heated at 80 °C to make it completely melt. Then the temperature raised 10 °C every 5 min to 180 °C and maintained for 1 h. In this process, caprolactam was hydrolyzed into amino acids. Self-condensation of the amino acids was originated at 200 °C for 2 h. The temperature was increased to 260 °C for further polycondensation and grafting reaction of PTCDA for 4 h. Equation of chemical reaction for synthesis of PA6/PTCDA composite was shown in Fig. 1. Finally the mixture was poured out from the flask and washed in boiling water for 5 h to remove the excess monomer or oligomers. The obtained polymers were vacuum dried for 6 h. Varied amounts of retardants ranged from 0.01 to 2.5 wt% were used for this study.

2.3 Characterization of PA6/PTCDA composites

PA6/PTCDA composites were placed in a vacuum oven at 90 °C for 12 h before Fourier-transform infrared (FTIR, Thermo Fisher Scientific, Nicolet iS50, USA) analysis. The composite and an appropriate amount of KBr were mixed by grinding and compressed into discs. XRD (BRUKER, D8 ADVANCE, Germany) was measured at a scanning speed of 8°/min with a continuous mode and at the range of 2θ within 8°–45°. To remove thermal history, the sample was heated to 100 °C under vacuum and then the sample was slowly cooled to room temperature before differential scanning calorimetry (Netzsch, DSC204F1, Germany) measurements. The DSC data was collected at a heating rate of 10 °C/min in a nitrogen atmosphere in the second cycle. The thermogravimetric analysis (Netzsch, STA449F3,

Fig. 1 The equation of chemical reaction for synthesis of PA6/PTCDA composite
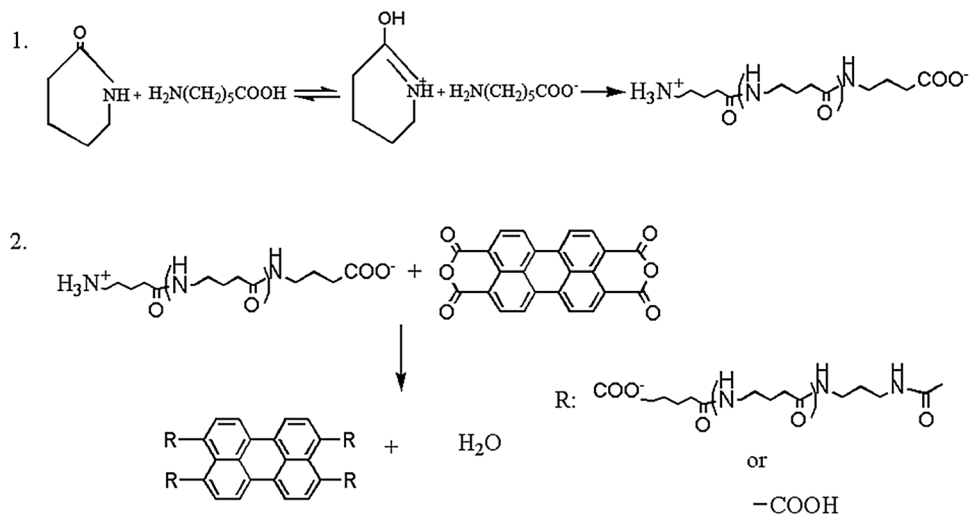
Germany) were measured under a nitrogen atmosphere from 25 to 800 °C with a heating rate of 10 °C/min. Limiting oxygen index values were tested by a digital oxygen index detector. Before the test, the sample was placed at 23 °C for at least 24 h, and then the sample was tested according to the GB/T2406.2-2009 standard. The λ of PA6/PTCDA blends was tested by a Netzsch LFA 447 Nanoflash at 25 °C. Each sample was tested five times to ensure the accuracy of the test. The density of the blends were measured by a full automatic densimeter (Ultrapycnometer1000). To obtain the intrinsic viscosity (η_{in}) of the blends the samples were dissolved in 85 wt% formic acid to make a uniform solution of 5 g/L, in an Ubbelohde viscometer at 30 °C. The Mark–Houwink equation $[\eta]_{in} = K(M_\eta)^\alpha$ (where $\alpha = 0.82$ and $K = 2.26 \times 10^{-4}$) was used to calculate the viscosity average molecular weight (M_η) [17].The Vertical burning test were tested by Horizontal and vertical combustion apparatus(ZR-02). After the sample was ignited, the first afterflame time t1 was recorded. Burning it again for 10 ± 0.5 s immediately when the afterflame extinguished, then the second afterflame time t2 and aferglow time t3 were recorded, respectively.

Fig. 2 Molecular weight and intrinsic viscosity of PA6/PTCDA

react with the amino group at the end of PA6 chain, which acts as the end-capping agent of PA6 chain, resulting in short PA 6 chains. Similar results were reported from an in situ polymerization approach to graphene-reinforced PA6 composites [18] and CNT-grafted polyurea composites [19].

3 Results and discussion

3.1 Molecular weight of PA6 and PA6/PTCDA composites

Figure 2 shows that the molecular weights of PA6/PTCDA decreased with increasing the feed fraction of PTCDA, from 21,605 g/mol for neat PA6 to 6962 g/mol for the PA6/PTCDA-2. The main reason is that the ratio of initiator to additive declined with the increasing of the additives, thus more macromolecules are formed with lower average molecular weight. PTCDA with anhydride group can
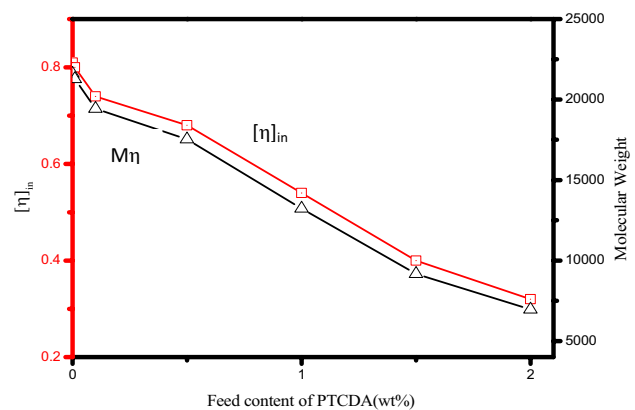
3.2 FTIR spectra of the composites

The characteristic peaks at 1570 cm^{-1}(N–H), 1650 cm^{-1}(C=O), 2940 cm^{-1}(CH2–) and 3400 cm^{-1}(N–H) in PA6/PTCDA composite were observed in Fig. 3. The broad band appearing at 1640 cm^{-1} corresponds to a stretching vibration of the amide functional group (-CONH-). As we all know, the absorption peaks at 1773 cm^{-1} and 1736 cm^{-1} were attributed to the characteristic peaks of the anhydride. However, these two characteristic peaks disappeared in PA6/PTCDA composite, indicating that the anhydride groups in PTCDA react with the terminated
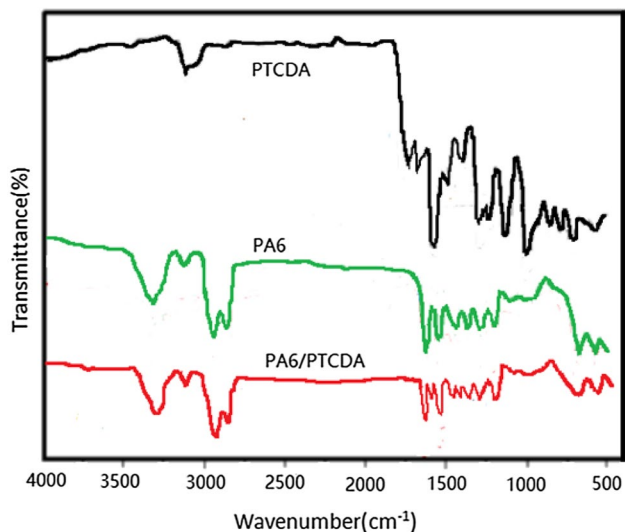
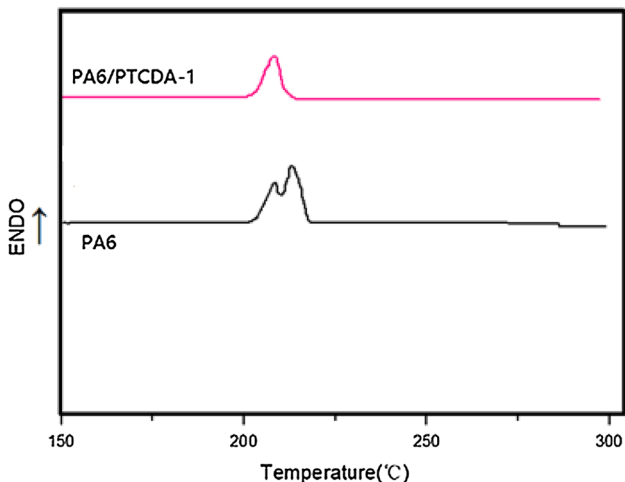**Fig. 3** FTIR spectra of PTCDA, PA6 and PA6/PTCDA composite

Table 1 Thermal conductivity (λ) of PA6 and PA6 composites

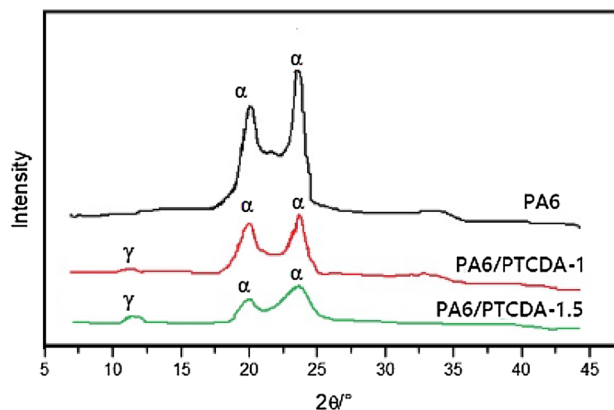| Sample	PA6	PA6/PTCDA-1
λ (W/(m K))	0.288	0.265
Density (g/cm^3)	1.21	1.19
Melting area (J/g)	72.47	68.23
T_m (°C)	215.8	211.3

Fig. 5 XRD patterns of PA6, PA6/PTCDA-1 and PA6/PTCDA-1.5

crystalline state of PA6 can be partly confirmed by measuring the density of PA6. The results of Roldan test and calculation show that PA6 with density of 1.229 g/cm^3, and 1.160 g/cm^3 tends to be α-crystal, and γ-crystal, respectively. When PTCDA is used as additive, the density changes from 1.21 g/cm^3 for PA6 to 1.19 g/cm^3 for PA6/PTCDA-1 (Table 1), suggesting the formation of more γ-crystal.

Figure 5 shows the XRD patterns of PA6 and PA6/PTCDA composites. The diffraction peaks located at 2θ of 20° and 24° correspond to (200) and (002, 202) reflections in α crystals of PA6 and PA6/PTCDA. With the addition of PTCDA, the diffraction peaks of the α crystal become weaker and wider, further evidencing for a depressed crystallization in PA6/PTCDA composites. In addition, the peak at 11.8° for γ crystal increases for the PA6/PTCDA composites, proving the formation of more γ crystal due to the influences of PTCDA.

Fig. 4 DSC curve of PA6 and PA6/PTCDA-1 composites

amino groups of PA6. It also illustrated the successful grafting reaction of PTCDA with PA6.

3.3 Characterization of thermal transition and crystallinity of the composites

The crystallization and thermal properties of PA6 and PA6/PTCDA composites were characterized by DSC as shown in Fig. 4. The peak of γ-crystals at 210 °C enhances and suppresses that of the α-crystal at 217 °C by adding PTCDA. Addition of PTCDA destroys the regularity of PA6 chains and enhances their activity. Meanwhile, PA6/PTCDA with lower molecular weight (Fig. 2) possesses faster crystallization rate, resulting in 'freezing' of the crystals and the decrease of the crystallinity. In addition, the internal

3.4 TGA curve of PA 6 and PA 6/PTCDA composites

Figure 6 shows the TGA curve of PA6 and PA6/PTCDA composites. The decomposition temperature of pure PA6 is about 375 °C. Because most of the chemical bonds in PA6 and PA6/PTCDA are similar, the initial decomposition temperature is not significantly different. However, before the decomposition of PA6, there is a mass loss for the PA6 composite, and the mass loss increases with the amount
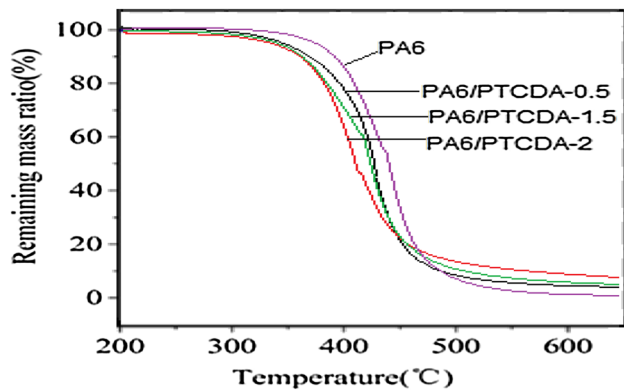
Fig. 6 Thermogravimetric curves of PA6 and PA6/PTCDA composites

Fig. 7 Limiting oxygen index values of PA6 with different content of PTCDA

of PTCDA, which can be contributed to the decomposition of carboxyl groups introducing by PTCDA. The thermal degradation temperature of PA6 is higher than that of PA6/PTCDA composites. The addition of PTCDA destroys the regularity of PA6 chain, making the molecular chain of PA6/PTCDA shorter, which will reduce the thermal stability of the material [20, 21]. In the 200–360 °C stage, the thermogravimetric curve of PA6/PTCDA is basically the same as those of pure PA6. The whole degradation process is one-step degradation. At 360–450 °C, the degradation rate of PA6 is faster than that of PA6/PTCDA. The increase of residual amount are mainly due to the addition of PTCDA to change the thermal degradation process of the material, promote the char forming ability of PA6/PTCDA, and slow down the thermal degradation ability of the material in the high temperature stage.

3.5 Flammability properties testing of composite materials

Limit oxygen index testing is an effective way to judge flammability properties of the materials. The relevant data are shown in Fig. 7. When 2.5% PTCDA is added, the LOI of the PA6/PTCDA increased to 29.5, which is much higher than that of neat PA6 (LOI 22.0). These data indicate that the addition of PTCDA can effectively enhance the combustion resistance of PA6 materials.

3.6 Flame retardancy mechanism

3.6.1 Test of thermal conductivity of composite materials

Generally, the thermal conductivity is related to the limiting oxygen index of the material. The higher the thermal conductivity, the faster the heat conduction of the material, results in the lower the remained heat, and the higher the limiting oxygen index. But by testing the thermal
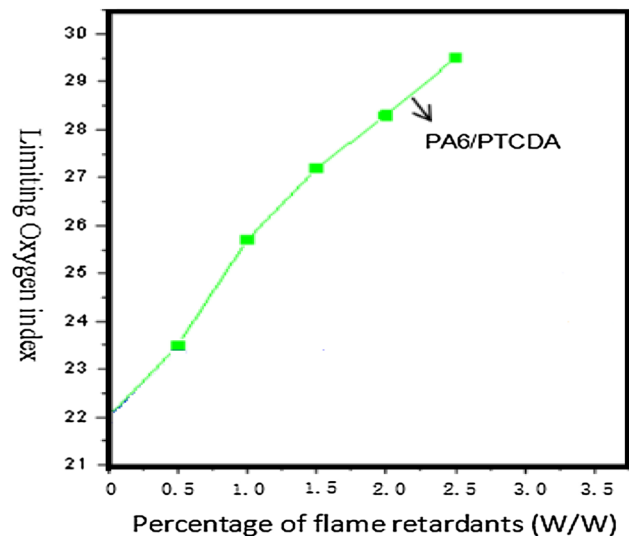
conductivity of the material (Table 1), the pure PA6 has a higher thermal conductivity than that of the PA6/PTCDA. However, the limiting oxygen index of PA6/PTCDA materials is higher than that of PA6, so the thermal conductivity of the PA 6 material is not the cause of the increase in the limiting oxygen index. So we simulated the real combustion process of the material to facilitate further exploration of the flame retardant mechanism of the material. The Cone calorimetry (CC) test data for the PA6 composites are summarized in Table 2 and Fig. 8. The heat release rate (HRR) curve of PA6/PTCDA is different from that of neat PA6. The peaks of the heat release rates of PA6 are higher than that of PA6/PTCDA composites. By comparing the specific extinction area and smoke yield data, PA6/PTCDA data is relatively small, indicating that the flame retardant mechanism of polymer is not gas phase flame retardant. The corresponding mean mass rate (mMLR) decreases from 0.150 g/s for PA6 to 0.062 g/s for PA6/PTCDA. PTCDA obviously reduces the rate of decomposition of the composite. These results indicate that PTCDA plays a role in the condensed phase [22].

The total heat release is one of the most important parameters to evaluate flame-retardant materials. The higher the total heat release is, the more heat the material will feed back to the surface when the material burns, which will increase the flame transmission ability of the material and the greater the risk of fire. It can be seen from Fig. 8b that the THR of PA6 is 89.24 MJ/m^2, which decreases to 70.23 MJ/m^2 after 2% PTCDA is added. It can be concluded that the addition of PTCDA can effectively reduce the total heat release of PA6 composites during combustion, greatly improving the safety of materials. The total

Table 2 Cone calorimetry (CC) test results for PA6 and PA6 composites

Sample	PA6	PA6/PTCDA (1%)	PA6/PTCDA (1.5%)	PA6/PTCDA (2%)
PHRR (kW/m²)	745.10	650.16	530.38	503.45
MHRR (kW/m²)	263.22	243.27	213.05	207.73
THR (MJ/m²)	89.24	82.17	74.01	70.23
PMLR (g/s)	0.35	0.27	0.19	0.15
MMLR (g/s)	0.15	0.098	0.062	0.054
TPHRR (S)	145	173	190	199
SEA (m²/kg)	80.25	82.09	82.19	84.53

PHRR peak heat release rate; *MHRR* mean heat release rate; *THR* total heat release; *PMLR* peak mass loss rate; *MMLR* mean mass loss rate; *TPHRR* time of peak heat release rate; *SEA* specific extinction area
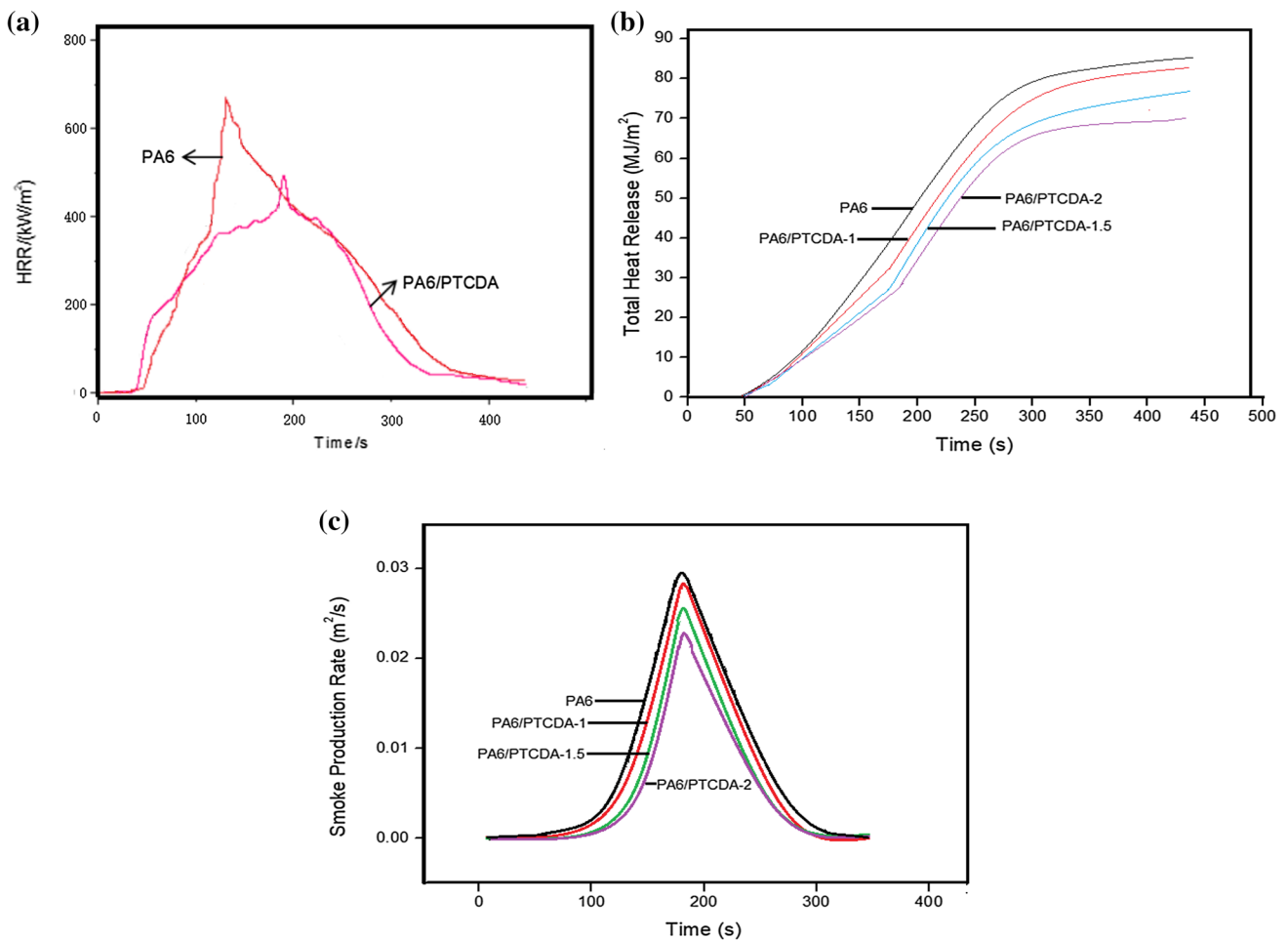

Fig. 8 Heat release rate (**a**), total heat release (**b**), and total smoke production rate (**c**) of PA6 and PA6 composites

amount of smoke produced (Fig. 8c) tends to decrease as the amount of PTCDA increases, and the smoke production rate of materials decreases from 0.028 to 0.022 m²/s at the same temperature, that is mainly due to the fact that a condensation layer will be formed on the surface of composites, which covers on the surface of the composite to reduce the smoke production.

3.6.2 Test of vertical burning of composite materials

The Vertical burning test results for PA6 and PA6 composites are shown in Table 3. The first and second afterflame time of PA6/PTCDA (1.5%) reduce 68.25%, and 75.84%, respectively, compare with that of PA6, which demonstrate that the addition of PTCDA can effectively shorten the time of

Table 3 Vertical burning test results for PA6 and PA6 composites

Sample	First after-flame time (s)	Second afterflame time (s)	Second aferglow time (s)	Combustion level
PA6	7.78	2.07	7.78	V-2
PA6/PTCDA (1%)	4.85	1.32	9.43	V-2
PA6/PTCDA (1.5%)	2.47	0.50	11.58	V-1
PA6/PTCDA (2%)	1.86	0.34	13.48	V-1

afterflame and improve the flame retardant performance of composites. However, the second afterglow time of PA6/PTCDA (1.5%) increases 48.84%. This is due to the formation of a stable char layer between the combustion area and non-combustion area during the burning process, thus protecting the flammable volatile components from being released. This char layer is believed to improve thermal stability and enhance flame retardant. The combustion level increases from V-2 level of PA6 to V-1 level of PA6/PTCDA (2%), indicating that the addition of PTCDA lowers the droplet temperature and improves the flame retardant performance of the composites.

4 Conclusions

PA6/PTCDA composites were prepared by in situ polymerization of caprolactam in the presence of PTCDA. PA6 was chemically modified by the polycondensation reaction between the anhydride functional groups contained in PTCDA and the amino functional groups containing PA6. When PTCDA are added, PA6 composite will produce new crystal form. In addition, with low amounts of PTCDA the limiting oxygen index of the PA6 composite can be improved, which effectively widens the field for the use of PA6. The properties of chemically modified PA6 provide a new way for the more extensive use of the material.

Compliance with ethical standards

Conflict of interest The authors declare that they have no competing interests.

References

1. Weil ED, Levchik SV (2009) Current practice and recent commercial developments in flame retardancy of polyamides. J Fire Sci 22:251–264. https://doi.org/10.1177/0734904104040546

2. Jang BN, Wilkie CA (2005) The effect of clay on the thermal degradation of polyamide 6 in polyamide 6/clay nanocomposites. Polymer 46:3264–3274. https://doi.org/10.1016/j.polymer.2005.02.078

3. Wang J, Olah A, Baer E (2016) Continuous micro-/nano-fiber composites of polyamide 6/polyethylene oxide with tunable mechanical properties using a novel co-extrusion technique. Polymers 82:166–171. https://doi.org/10.1016/j.polymer.2015.11.035

4. Monticelli O, Musina Z, Frache A, Bellucci F, Camino G, Russo S (2007) Influence of compatibilizer degradation on formation and properties of PA6/organoclay nanocomposites. Polym Degrad Stabil 92:370–378. https://doi.org/10.1016/j.polymdegradstab.2006.12.010

5. Butnaru I, Fernandez-Ronco MP, Czech-Polak J, Heneczkowski M, Bruma M, Gaan S (2016) Effect of meltable triazine-DOPO additive on rheological, mechanical, and flammability properties of PA6. Polymers 7:1541–1563. https://doi.org/10.3390/polym7081469

6. Chen L, Wang YZ (2010) A review on flame retardant technology in China. Part I: development of flame retardants. Polym Adv Technol 21:1–26. https://doi.org/10.1002/pat.1550

7. Kudashev SV, Medvedev VP (2018) Composites of reduced flammability based on amorphous elastic polyurethane and halogen-containing flame retardant. Russ J Appl Chem 91:520–523. https://doi.org/10.1134/S1070427218030266

8. Mu JQ, Yang Y, Peng ZH (2011) Preparation and characterization of a novel flame retard-ed MCA-PA6 resin by in situ polymerization. Adv Mater Res 399:444–448. https://doi.org/10.4028/www.scientific.net/AMR.399-401.444

9. Hu Y, Wang S, Ling Z, Zhuang Y, Chen Z (2003) Preparation and combustion properties of flame retardant nylon 6/montmorillonite nanocomposite. Macromol Mater Eng 288:272–276. https://doi.org/10.4028/www.scientific.net/AMR.399-401.444

10. Fei GX, Liu Y, Wang Q (2008) Synergistic effects of novolac-based char former with m-agnesium hydroxide in flame retardant polyamide-6. Polym Degrad Stabil 93:1351–1356. https://doi.org/10.1016/j.polymdegradstab.2008.03.031

11. Alongi J, Poskovic M, Visakh PM, Frache A, Malucelli G (2012) Cyclodextrin nanosponges as novel green flame retardants for PP, LLDPE and PA6. Carbohydr Polym 88:1387–1394. https://doi.org/10.1016/j.carbpol.2012.02.038

12. Xu YS, Ray G, Abdel-Magid B (2006) Thermal behavior of single-walled carbon nanotube polymer-matrix composites. Compos A Appl Sci 37:114–121. https://doi.org/10.1016/j.compositesa.2005.04.009

13. Li X, Shao L, Song N, Shi L, Ding P (2016) Enhanced thermal-conductive and anti-dripping properties of polyamide composites by 3D graphene structures at low filler content. Compos A Appl Sci 88:305–314. https://doi.org/10.1016/j.compositesa.2016.06.007

14. Krause B, Durr AC, Ritley K, Schreiber F (2002) Structure and growth morphology of an archetypal system for organic epitaxy: PTCDA on Ag(111). Phys Rev B 66:126–130. https://doi.org/10.1103/PhysRevB.66.235404

15. Zeng C, Lu S, Xiao X, Gao JLP (2015) Enhanced thermal and mechanical properties of epoxy composites by mixing noncovalently functionalized graphene sheets. Polym Bull 72:453–472. https://doi.org/10.1007/s00289-014-1280-5

16. Iqbal R, Khosa MK, Jamal MA, Hamid M (2015) Synthesis and thermal properties of polyimides containing azomethine linkage for processable high-performance engineering plastics. Korean J Chem Eng 32:362–368. https://doi.org/10.1007/s11814-014-0205-1

17. Xu Z, Gao C (2010) In situ polymerization approach to graphene-reinforced nylon-6 composites. Macromolecules 43:6716–6723. https://doi.org/10.1021/ma1009337

18. Hou WJ, Tang BQ, Lu LL, Sun J, Wang JJ, Qin CX, Dai LX (2014) Preparation and physico-mechanical properties of amine-functionalized graphene/polyamide 6 nanocomposite fiber as a high performance material. RSC Adv 4:4848–4855. https://doi.org/10.1039/c3ra46525j

19. Gao C, Jin YZ, Kong H, Whitby RL, Acquah SF (2005) Polyurea-functionalized multiwalled carbon nanotubes: synthesis, morphology, and Raman spectroscopy. J Phys Chem B 109:11925–11932. https://doi.org/10.1021/jp051642h

20. Hojabri L, Jose J, Leao AL, Bouzidi L, Narine SS (2012) Synthesis and physical properties of lipid-based poly(ester-urethane)s, I: effect of varying polyester segment length. Polymer 53:3762–3771. https://doi.org/10.1016/j.polymer.2012.06.011

21. Yang HK, Zhao H, Yang PR, Huang CH (2017) How do molecular structures affect gelation properties of supramolecular gels? Insights from low-molecular-weight gelators with different aromatic cores and alkyl chain lengths. Colloid Surf A 535:242–250. https://doi.org/10.1016/j.colsurfa.2017.09.044

22. Sahyoun J, Bounor-Legare V, Ferry L (2015) Synthesis of a new organophosphorous alkoxysilane precursor and its effect on the thermal and fire behavior of a PA66/PA6 copolymer. Eur Polym J 66:352–366. https://doi.org/10.1016/j.eurpolymj.2015.02.036